LA-UR- 98-3059

Approved for public release; distribution is unlimited.

Title: HIGH-AND-LOW-STRAIN RATE, COMPRESSION OF SEVERAL ENERGETIC MATERIAL COMPOSITES AS A FUNCTION OF STRAIN RATE AND TEMPERATURE

CONF-980803--

Author(s): G.T. GRAY III, MST-8
D.J. IDAR, DX-2
W.R. BLUMENTHAL, MST-8
C.M. CADY, MST-8
P.D. PETERSON, DX-2

Submitted to: 11th INTERNATIONAL DETONATION SYMPOSIUM
AUG. 31-SEP 4, 1998
SNOWMASS VILLAGE, CO

Los Alamos
NATIONAL LABORATORY

DISCLAIMER

DISCLAIMER

Portions of this document may be illegible in electronic image products. Images are produced from the best available original document.

HIGH- AND LOW-STRAIN RATE COMPRESSION PROPERTIES OF SEVERAL ENERGETIC MATERIAL COMPOSITES AS A FUNCTION OF STRAIN RATE AND TEMPERATURE

G.T. Gray III, D. J. Idar, W.R. Blumenthal, C.M. Cady, and P. D. Peterson

Los Alamos National Laboratory
Los Alamos, New Mexico 87545

High- and low-strain rate compression data were obtained on several different energetic composites: PBX 9501, X0242-92-4-4, PBXN-9, as well as the polymeric binder used in PBX 9501 and X0242-92-4-4 composites. The effects of energetic-to-binder ratios, different binder systems, and different energetic formulations were investigated. All the energetic composites exhibit increasing elastic modulus, E, maximum flow stresses, σ_m, and strain-at-maximum stress, ε_m, with increasing strain rate at ambient temperature. PBX 9501 displays marginally higher ultimate flow strength than X0242-92-4-4, and significantly higher ultimate compressive strength than PBXN-9 at quasi-static and dynamic strain rates. The failure mode of PBX 9501 and X0242-92-4-4 under high-rate loading changes from a mixture of ductile binder tearing and transgranular cleavage and cracking of the HMX when tested at 20°C to transgranular brittle HMX cleavage and glassy fracture of the binder at –40°C.

INTRODUCTION

Munitions and propellant safety concerns in recent years have motivated significant experimental and modeling efforts to develop physically-based constitutive models for modern energetics and propellants. Models are needed to predict the mechanical behavior, damage evolution and fracture initiation, response thresholds, and performance of energetic materials for their safe usage in current and future engineering applications. Low-level insults, ranging from accidental handling impacts, setback loads, to more intense collateral damage, may cause delayed transition to detonation, termed XDT, in granular propellant or damaged explosives. Since the pioneering work of Bowden et. al.[1,2] explored how impact and frictional processes can lead to "hot spots", numerous researchers[3-6] have examined mechanically-driven ignition of explosives and propellants. Indeed, the widespread observance of mechanically-induced impact ignition led to the adoption of a spectrum of drop-weight and/or impact experimental techniques to characterize and quantify energetic and propellant impact sensitivity.[7-10] Not withstanding the significant experimental insights that have been elucidated in this area, the fundamental physical micromechanisms controlling mechanically-induced ignition and the first-principles modeling of these processes remains poorly understood. The development of robust constitutive models of mechanically-induced (non-shock prompt) ignition requires quantification of: 1) the stimulus (stress-strain state, confinement, strain rate, and temperature) required for initiation to detonation or violent reaction, 2) scale effects (i.e. the effect of explosive failure dimensions and geometry on initiation versus quenching processes), and 3) microstructural variables (energetic crystal morphology and size, binder interactions, etc.) that affect homogeneous and heterogeneous initiation mechanisms.

The complex interactions and synergisms existing between the pure constitutive response, loading history and damage evolution, and potential fracture processes in energetics and propellants prior to ignition further complicate this list of relevant research topics.

Modeling of mechanically-triggered ignition of plastic-bonded explosives (PBXs) first requires a description of the time and temperature dependency of the stress-strain response of the energetic or propellant of interest for any given history of elastic, viscoelastic, and/or viscoplastic flow. A number of previous studies have probed the constitutive response of a wide variety of PBXs[5,11-16]. The high-rate studies of Hoge,[13]

Field,[5,11] Palmer,[14] and Walley (Reference #?) have shown that: a) the effective elastic modulus of PBXs are strongly influenced by strain rate and temperature, b) PBXs during high-rate loading continue straining after the maximum flow stress has been achieved, i.e. visco-elastic-plastic behavior is indicated, and c) specimen geometry and lubrication effects are important due to the slow wave propagation through PBXs and their susceptibility to shear localization and failure. Low-strain-rate studies on PBXs by Peeters,[15] Wiegand[16] and Funk[12] have similarly shown that the compressive strength (maximum stress) and the loading modulus increase with decreasing temperature and increasing strain rate. Wiegand[16] has further demonstrated a linear correlation between compressive strength and modulus independent of loading rate in compression or temperature, for a range of PBXs. This behavior, observed over a range of strain rates, suggests a critical resolved tensile strain criterion to initiate brittle fracture, similar to ceramics.

This paper describes research that systematically measured the influence of variations in the applied strain rate, from quasi-static to dynamic, and temperature on the mechanical response of three PBX-based energetics: PBX 9501, X0242-92-4-4, PBXN-9, and also the binder material for PBX 9501 and X0242-4-4. The fracture surfaces of PBX 9501 and X0242-92-4-4 specimens, as a function of temperature, were also probed using Scanning Electron Microscopy (SEM).

EXPERIMENTAL

Materials

This investigation was performed on three HMX-based plastic-bonded explosives: PBX 9501, X0242-92-4-4 (hereafter referred to as X0242), PBXN-9, and the Estane 5703 / nitroplasticizer binder (hereafter referred to as the PBX 9501 binder) utilized in PBX 9501 and X0242. The HMX and binder weight percentages for these compositions are given for reference in Table 1. The various specimen average densities with standard deviations from measurement-to-measurement are also given. These are expressed in units of mass per volume and as percentages relative to the theoretical maximum density (%TMD) for each of the compositions. These data reveal that the PBXN-9 specimens, on average, had the highest percentage of the theoretical maximum density, and X0242 the lowest.

PBX 9501 is a formulation composed of respectively, 94.9 / 2.5 / 2.5 / 0.1 wt% of HMX / 5703 Estane / a eutectic mixture of bis(2,2 dinitropropyl)acetal and bis(2,2-dinitropropyl)formal [abbreviated BDNPA-F] / and a free radical inhibitor (either diphenylamine (DPA) or Irganox). The PBX 9501 sample chosen for this study contained the Irganox free radical inhibitor.

The HMX in PBX 9501 is composed of a three-to-one ratio of coarse-to-fine grades of HMX. The coarse grade is class 1 HMX with a range of particulate sizes primarily between 44 and 300 microns. The fine grade Class 2 HMX also has some large particulates, but at least 75% of the sizes are 44 microns or less. This bimodal size distribution contributes to a higher packing density under heated, isostatic pressing conditions.

The Estane 5703 is an amorphous, thermoplastic polyester polyurethane with a glass transition temperature (T_g) of –31°C.[new B. F. Goodrich reference] The bulky copolymer backbone is composed of soft and hard segments that enhance entanglement. Estane is known for its resistance to hydrocarbon and solvent attack, low temperature flexibility, high temperature resistance, and good adhesive properties. The high strength of the copolymer is associated with its 'virtual crosslinking' attributed to both molecular entanglement and intermolecular forces (i.e. hydrogen bonding, van der Waals, and polar attraction) concentrated at the ester linkages. The addition of the BDNPA-F plasticizer causes the polymer strength to decrease, but the toughness and flexibility are increased. The plasticizer acts as a 'lubricant' to promote the sliding of the polymer chains, and to reduce the degree of entanglement. This in turn reduces the glass transition temperature for the binder and composite material.

X0242 is a formulation comprised of the exact same constituents as PBX 9501, but with ~3 wt% less HMX, and 4 wt% each of 5703 Estane and BDNPA-F. The same ratio of coarse-to-fine grades of HMX is used in

TABLE 1: HE AND BINDER WEIGHT % AND AVERAGE DENSITY OF HE SPECIMENS

Formulation/HE	HE (wt%)	Binder (wt%)	Average Density (g/cm^3) (% TMD)
PBX 9501	94.9% HMX 3 to 1 Class 1: 2	2.5% Estane 2.5% BDNPA-F 0.1% Irganox	1.827 ± 0.003 (98.2%)
X0242-92-04-04	92% HMX 3 to 1 Class 1: 2	4.0% Estane 4.0% BDNPA-F	1.807 ± 0.005 (97.7%)
PBXN-9	92% HMX 1.2 to 1 Class 1:5	2.0% HyTemp 4454 (Hycar 4454), 6.0% dioctyl adipate	1.748 ± 0.011 (99.1%)

X0242 as well. The PBX 9501 and X0242 molding powders were prepared by the slurry mixture method containing the HMX crystals and binder. The dried powder was then preheated and pressed into a billet form with two or more compaction loading cycles to achieve the desired density.

PBXN-9 is composed of 92 wt% HMX, similar to X0242, however with a different bimodal ratio of 1.2-to-1 coarse-to-fine grades of HMX and a different binder. The coarse grade class 1 HMX is the same as that used for PBX 9501 and X0242, but the fine grade, class 5, has at least 98% particulates in the range of 44 microns or less. This may contribute to a more efficient packing density during compaction and a higher %TMD for the PBXN-9. The smaller number of large particulates may also lower the percentage of stress bridging in the composition under compression relative to the PBX 9501 and X0242 materials, and reduce the level of transgranular cleavage in failure. A completely different binder is also used in the PBXN-9 formulation which is composed of 2.0 wt% HyTemp 4454 (Hycar 4454) and 6.0 wt% dioctyl adipate (DOA) plasticizer. The HyTemp 4454 elastomer is contains a less complex, polybutyl acrylate backbone and behaves similar to unvulcanized rubber. It is also known for its heat resistance and low glass transition temperature of –40°C.(new Navy report reference) DOA is derived from adipic acid and causes more 'softening' of the PBXN-9 due to the higher 3-to-1 wt% ratio of plasticizer-to-elastomer in the binder.

Billets of the PBX 9501 and X0242 were pressed at Los Alamos National Laboratory (LANL), and the PBXN-9 was obtained from a Navy source. Compression specimens for the low- and high-strain-rate tests were machined from these pressed billets in a compression orientation parallel to the billet pressing direction. Due to the normally soft and visco-elastic nature of the binder materials, a specialized machining procedure was developed to maintain parallel loading surfaces. Adequate rigidity during machining was achieved by carefully cooling the specimen with a controlled spray of liquid nitrogen during machining.

Low Strain Rate Compression Testing

Quasi-static compression tests were conducted at strain rates of 0.0011, 0.011, 0.11, and 0.44 s^{-1} at ~25°C in ambient temperature air exhibiting a relative humidity ranging from 26% to 48% using either a screw-driven Instron Corp. (Canton, MA) 1123 or 5567 Materials Testing Workstation. Load and strain measurements were obtained with an Instron load cell and extensometer placed directly between the loading platens adjacent to the compression specimen. All of the HE specimens were approximately 9.5 mm diameter by 19 mm long. All tests were conducted with lubrication (dry film graphite lubricant on the platens, and a thin layer of molybdenum disulfide on the specimens). Averages and standard deviations were determined from five repetitions per condition.

High Strain Rate Compression Testing

Cylindrical compression specimens 6.35 mm in diameter and either 6.35 mm or 3.15 mm in length (L/D of 1 or 0.5) were machined for the high-strain-rate testing. Dynamic tests were conducted as a function of strain rate, 1700-2800 s^{-1}, and temperature, -55°C to +55°C, utilizing a split-Hopkinson pressure bar (SHPB). The SHPB used for this study was equipped with either 9.4-mm diameter Ti-6Al-4V or Magnesium AZ31B-alloy bars that improve the signal-to-noise level needed to test extremely low strength materials as compared to the maraging steel bars traditionally utilized for SHPB studies on metals. The lower sound speed titanium and magnesium bars also help achieve sample stress equilibrium sooner, but because of the inherent oscillations in the dynamic stress-strain curves and the lack of stress equilibrium during initial load-up, the determination of yield strength must be considered inaccurate, at best, at high strain rates.

Controlled test temperatures between –55°C and +55°C on the SHPB were achieved utilizing a specially-designed gas manifold system developed at LANL where specimens were cooled and heated using helium (He) gas within a 304-stainless steel containment chamber held at a partial vacuum.[17, 18] The He gas is cooled below ambient temperature by first passing the He through a copper coil positioned within a liquid nitrogen dewar, while elevated temperatures are achieved by remotely heating the He in a similar coil immersed in glycerin-filled beaker heated to ~200°C by a heating plate. Specimens were lubricated using either a thin layer of molybdenum disulfide grease or a boron nitride spray lubricant.

RESULTS AND DISCUSSION

The compressive true-stress versus true-strain responses of PBX 9501, X0242, PBXN-9, and the PBX 9501 binder were all found to depend on the applied strain rate, varied between 0.0011 and 2800 s^{-1}, and the test temperature, varied between –55°C and +55°C at strain rates of 1700-2800 s^{-1}. Note that the density of the three compositions given in Table 1 ranges from 97.7 to 99.1 %TMD. Assuming that porosity accounts for the difference from theoretical density, these three materials do not contain the same bulk porosity level. Even though the porosity levels and variations between materials are slight, this property may have a

consequential effect on the viscoelastic, viscoplastic and failure mode behavior. However, the data and analysis reported herein are insufficient to evaluate this effect. Nonetheless, it is important to be aware that porosity is known have a significant effect on the mechanical behavior of high explosive (HE) formulations and can play a key role in the ignition/reaction sequence under low amplitude mechanical loading.

Quasi-Static Stress-Strain

Figures 1a-c present the quasi-static ambient temperature (~25°C) compressive stress-strain behavior of PBX 9501, X0242, and PBXN-9 as a function of strain rate. The quasi-static maximum flow stress (σ_m), the strain-at-maximum stress value (ε_m), and the elastic modulus (E) are summarized in Table 2. The standard deviation and the relative percent deviation (in parenthesis) are also presented in Table 2 for each parameter (σ_m, ε_m, and E). An evaluation of these plots and the data in Table 2 reveals: 1) PBX 9501 displays a somewhat higher ultimate flow strength than X0242, and significantly higher ultimate compressive strength than PBXN-9, 2) X0242 displays a substantially slower fall-off in flow stress after its maximum flow strength than either PBX 9501 or PBXN-9, 3) PBX 9501 exhibits the lowest strain-at-maximum-stress values, and 4) all three stress-strain parameters (E, σ_m, and ε_m) increase with strain rate.

The differences between the pristine mechanical properties of PBX 9501, X0242, and PBXN-9 are not surprising based on their compositions. Qualitatively the PBXN-9 has a pliable, gum-eraser-like consistency as compared to the PBX 9501 and X0242 that are much stiffer and "wax-like". The PBX 9501 and PBXN-9 formulations, representing the extreme cases, exhibit several key differences: a) the overall binder content is higher and the "hard" HMX phase content is lower in PBXN-9; b) the HyTemp 4454 used in PBXN-9 has a lower Tg than the Estane; c) the ratio of plasticizer to elastomer is higher in the PBXN-9 which contributes to a lower T_g; and d) the HMX particulate size distribution of PBXN-9 contains more fines which reduces stress bridging.

Mechanical Response of PBX 9501 Binder

In addition to the PBX composites, the constitutive response of the binder utilized in PBX 9501 (1:1 Estane/BDNPA-F) was separately studied quasi-statically and at high strain rate as shown in Figure 2. An understanding of the influence of temperature and strain rate on individual constituents of PBX composites is needed to support robust constitutive-model development on a range of PBX formulations. The stress-strain data from the PBX 9501 binder demonstrates: 1) the very low overall flow strength of this nitroplasticized binder compared to the composite PBX 9501, 2) the order of magnitude increase in the binder flow stress when the test temperature is lowered from ambient to -20°C at high-strain rate, and 3) the equally large increase in the binder flow strength associated with increasing the strain rate.

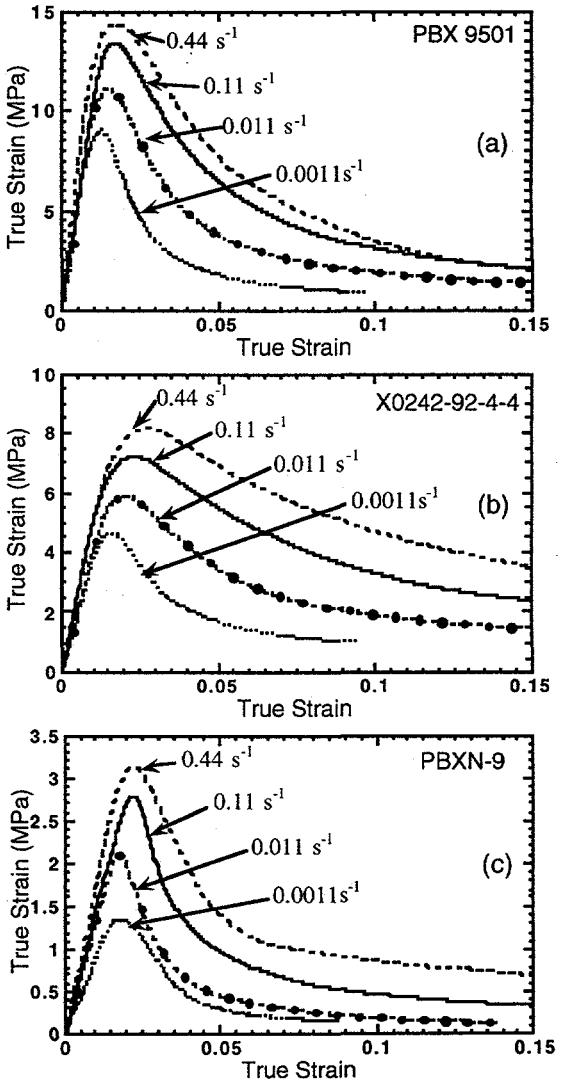

FIGURE 1. AVERAGE STRESS-STRAIN DATA FOR A) PBX 9501, B) X0242-92-4-4, AND C) PBXN-9 WITH L/D = 2.

Validity of SHPB Testing of Energetics

Due to the previously demonstrated dispersive nature of wave propagation in ductile polymers[18] and

plastic-bonded energetics[17] the high-rate constitutive response of PBX 9501, X0242, PBXN-9, and the PBX 9501 binder was carefully probed to assure valid and accurate SHPB data.

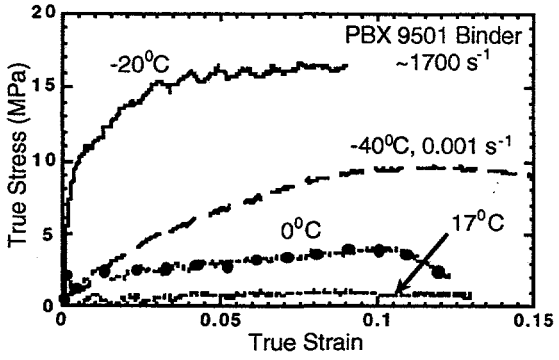

FIGURE 2. TRUE STRESS-STRAIN DATA FOR PBX 9501 BINDER (1:1 Estane/BDNPA-F) AT ~1700 s^{-1} AND –40°C @ 0.001 s^{-1}.

To verify the high-rate SHPB measurements different analyses[19] were used to calculate specimen stress from the three SHPB bar strains as illustrated in Figure 3. In the 1-wave analysis the specimen stress is directly proportional to the bar strain measured from the transmitted bar. The 1-wave stress analysis reflects the conditions at the specimen-transmitted bar interface and is often referred to as the specimen "back stress". This analysis results in more accurate and smoother stress-strain curves, especially at low strains near yield. Alternatively, the 2-wave analysis uses the sum of the synchronized incident and reflected bar waveforms (opposites in sign) to calculate the specimen "front stress" which reflects the conditions at the incident/reflected bar-specimen interface. A valid, uniaxial stress SHPB test requires that the stress state throughout the specimen achieve equilibrium during the test and this condition can be checked readily by comparing the 1-wave and 2-wave stress-strain response. When the stress state is uniform throughout the specimen, then the 2-wave stress oscillates about the 1-wave stress. Attainment of stress state equilibrium at high-strain rates was also found to be dependent on the test temperature. Specifically, at low test temperatures polymer specimens equilibrate more quickly because their stiffness (i.e. sound speed) increases significantly.

TABLE 2: AVERAGE σ_m, ε_m, AND E VALUES WITH STANDARD DEVIATION, TEST TEMPERATURE, AND RELATIVE HUMIDITY (RH%), AT LOW-STRAIN RATES FOR PBX 9501, X0242-92-04-04 (X0242), AND PBXN-9.

HE TYPE	Strain Rate (s^{-1})	σ_m (MPa)	ε_m	E (MPa)	Temperature (°C)	% RH
PBX 9501	0.0011	9.05±0.36 (4.0%)	0.0129±0.0007 (5.4%)	956.9±85.2 (8.9%)	26.9±0.8	38.3±3.4
PBX 9501	0.011	11.11±0.48 (4.3%)	0.0148±0.0008 (5.4%)	1015.5±110.5 (10.9%)	26.6±1.9	39.6±9.1
PBX 9501	0.11	13.35±0.39 (2.9%)	0.0167±0.0005 (3.0%)	1085.1±44.0 (4.1%)	27.0±0.1	39.3±0.4
PBX 9501	0.44	14.53±0.37 (2.6%)	0.0188±0.0008 (4.3%)	1151.5±109.5 (9.5%)	25.1±0.4	48.0±0.9
X0242	0.0011	4.68±0.22 (4.7%)	0.0168±0.0012 (7.1%)	360.4±32.4 (9.0%)	28.1±0.2	30.8±1.2
X0242	0.011	5.96±0.20 (3.4%)	0.0198±0.0005 (2.5%)	408.9±15.6 (3.8%)	25.7±0.6	41.9±2.4
X0242	0.11	7.24±0.16 (2.2%)	0.0229±0.0003 (1.3%)	454.4±27.1 (6.0%)	27.3±0.1	43.1±2.8
X0242	0.44	8.28±0.25 (3.0%)	0.0260±0.0018 (6.9%)	515.1±59.6 (11.6%)	25.9±0.1	46.0±0.1
PBXN-9	0.0011	1.35±0.03 (2.2%)	0.0180±0.0012 (6.7%)	88.5±6.6 (7.5%)	24.6±0.3	28.6±0.7
PBXN-9	0.011	2.07±0.09 (4.3%)	0.0186±0.0013 (7.0%)	122.8±12.0 (9.8%)	25.1±0.1	27.6±0.4
PBXN-9	0.11	2.72±0.18 (6.6%)	0.0218±0.0011 (5.0%)	135.6±13.6 (10.0%)	25.5±0.3	27.1±0.5
PBXN-9	0.44	3.12±0.02 (0.6%)	0.0222±0.011 (5.0%)	169.4±9.2 (5.4%)	25.5±0.1	26.7±0.3

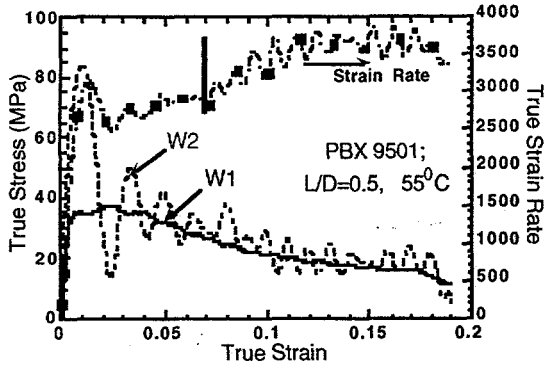

FIGURE 3. STRESS-STRAIN RESPONSE OF PBX 9501 SHOWING 1-WAVE AND 2-WAVE STRESS CURVES AND STRAIN RATE VERSUS STRAIN.

Accordingly, the "worse-case" condition for the evaluation of SHPB specimen L/D is at high temperatures.[17] Viscoelastic effects are pronounced in the PBX 9501 at 55°C, as seen in Figure 3, and approximately 2% strain is needed before stress-state equilibrium is achieved. Through comparisons of this type, it was determined that a specimen aspect ratio of L/D=0.5 is optimum for achieving valid test data for the energetics and binder studied. Only tests meeting all of the criteria discussed were deemed valid.

Finally, the achievement of a reasonably constant strain rate is also deemed necessary for obtaining quantitative constitutive data suitable for modeling and as an indicator of deleterious inertial effects such as specimen failure. To illustrate, the strain rate-strain plot in Figure 3 is reasonably constant between strain values of 2% to 6%. Thereafter, the strain rate increases which was found to coincide with macroscopic fracture of the specimen, albeit the 1-wave and 2-wave stress-strain curves still appears to be in equilibrium (although steadily decaying). Therefore, the composite plots in Figure 3 demonstrate the crucial importance of carefully monitoring and utilizing 1-wave stress, 2-wave stress, and strain rate versus strain analysis during **ALL** SHPB tests to validate specimen stress-state equilibrium and to help define the transition from deformation to failure. During specimen failure the strain rate-strain plot provides unique information not present in the 1-wave or 2-wave stress-strain plots.

High Strain Rate Response of PBX 9501, X0242, and PBXN-9

Figure 4 displays the high strain rate behavior of the three energetics as a function of temperature. Analysis of this data for PBX 9501, X0242, and PBXN-9 presents a number of key similarities and differences. First the yield strengths of PBX 9501, X0242, and PBXN-9 were all found to be strongly dependent on temperature. This trend is consistent with the pronounced influence of strain rate and temperature on the mechanical behavior of other energetics[13] as well as ductile polymers[20] and the currently evaluated PBX 9501 binder. Second, similar to the quasi-static data presented earlier, PBX 9501 displays the most pronounced fall-off in flow stress following its maximum flow strength compared to X0242, or PBXN-9. This trend is directly consistent with the amount of binder present in each energetic where a higher binder content produces a more "ductile" response.

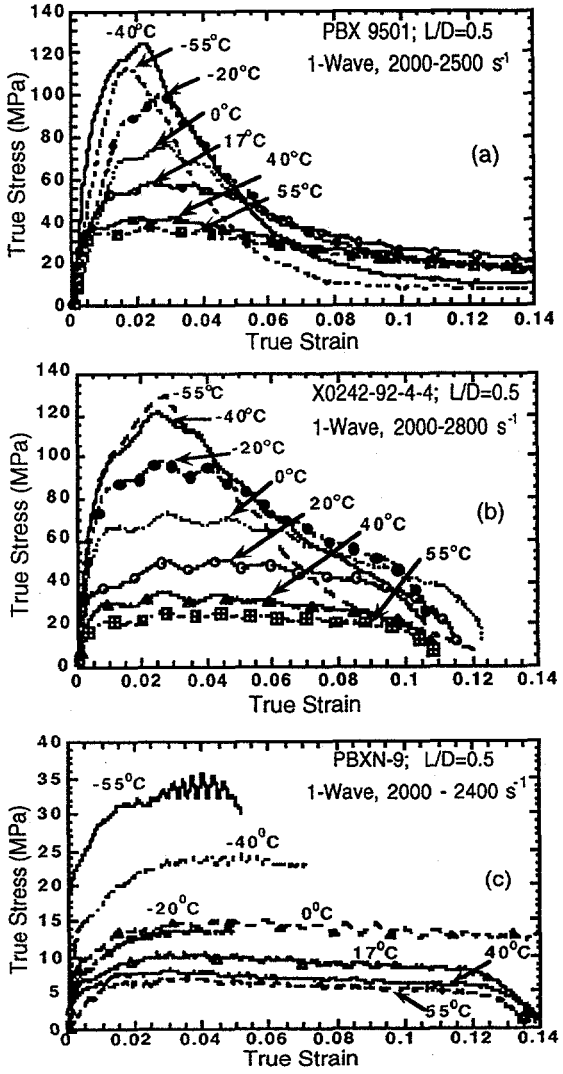

FIGURE 4. HIGH-STRAIN-RATE TRUE STRESS-STRAIN DATA FOR A) PBX 9501, B) X0242-92-4-4, AND C) PBXN-9.

Third, PBXN-9, which contains the same total binder fraction as X0242 but with three times the plasticizer-to-elastomer ratio, did not fracture during high-rate/low temperature testing and displayed substantially lower flow stress levels than the PBX 9501 or X0242 consistent with the quasi-static results of Figure 1. Finally, the stress-strain curve for PBX 9501 at –55°C in Figure 4a lies slightly below the data for –40°C which suggests the intervention of brittle fracture prior to the achievement of uniform yielding. This postulation is supported by the combined 1-wave and 2-wave stress analysis which shows that stress-state equilibrium was not fully achieved prior to the fall-off in the flow stress.

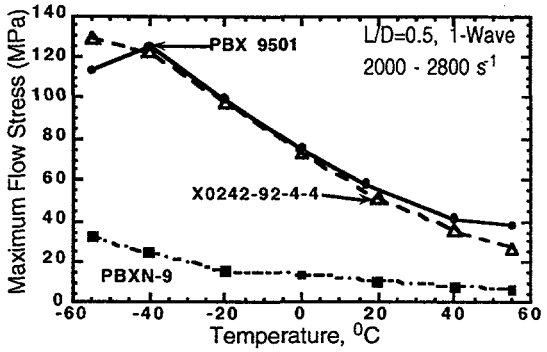

FIGURE 5. HIGH STRAIN RATE MAXIMUM FLOW STRESS VERSUS TEMPERATURE FOR PBX 9501, X0242-92-4-4, AND PBXN-9.

The temperature dependence of the maximum flow stress for the three energetics at high strain rates is summarized in Figure 5. In the range of about –40°C to +40°C all three energetics display a relatively linear dependence of maximum strength on test temperature. However, at the extreme temperatures of –55°C and +55°C the response of PBX 9501 and X0242 is seen to deviate significantly from linearity. At –55°C the PBX 9501/X0242 binder is below its glass-transition temperature, so that the deviation from linearity may be related to a change from ductile flow to brittle cracking of the binder. At +55°C, the decline in the maximum flow stress of X0242 and PBX 9501 with temperature diminishes and disappears, respectively. This behavior is likely due to the loss of strength and adhesion of the binder. Note that a correction for the slight %TMD difference between PBX9501 and X0242 (see Table 1) will bring the high strain rate flow strengths even closer together between –40°C and +40°C.

In the case of PBXN-9 where the glass transition temperature of the binder is below –55°C, the temperature dependence of the maximum flow stress actually increases below –20°C. Also considering the identical HMX content (92 wt%) in both PBXN-9 and X0242, the greater than a factor of two difference in flow strength at both low- and high strain rates dramatically demonstrates the importance of binder properties and HMX particulate size distribution on the stress-strain response of energetics.

Coincident with the flow stress increase upon decreasing the temperature is a significant increase in the apparent loading modulus with decreasing temperature at high strain rates consistent with previous studies on PBX 9501[21] and other energetics.[15,16] In addition, the strain-at-maximum-stress was observed to be largely temperature invariant, similar to the findings of Wiegand[16] for various PBXs, and was correlated to the binder content and binder formulation. Specifically, the strain-at-maximum stress was ~2% for PBX 9501, ~3% for X0242, and ~4% for PBXN-9. This behavior supports the theory that failure during "nominally uniaxial" compression loading is actually driven by a critical tensile initiation criterion.

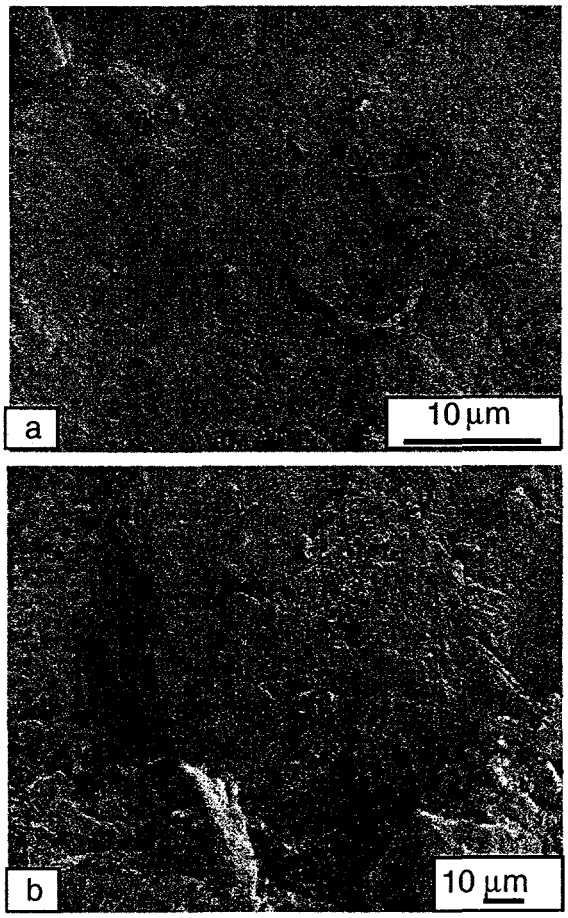

FIGURE 6. SEM FRACTOGRAPH OF PBX 9501 FOLLOWING SHPB TESTING AT A STRAIN RATE OF 2000 s^{-1}: A) 17°C, B) –40°C.

Details of the damage and failure behavior of PBX 9501 and X0242 specimens following high strain rate testing were examined via fractographic analysis using a scanning electron microscope (SEM). SEM of SHPB compression specimens tested at 17°C and –40°C revealed that both energetics exhibited temperature-dependent microstructural damage accumulation prior to macroscopic failure. A PBX 9501 specimen which failed at 17°C exhibited both transgranular fracture through the HMX crystals and a mixture of ductile tearing and low-strain binder failure, as seen in Figure 6a. Upon decreasing the test temperature to –40°C, the predominant failure mode was brittle fracture through the HMX crystals and glassy binder fracture, as seen in Figure 6b. The observation of predominantly transgranular fracture in PBX 9501 is similar to that seen following quasi-static loading.[16] These observations point to the need for advanced energetic material models which incorporate the influence of strain rate and temperature on both stress-strain constitutive response and damage evolution-based failure processes.

CONCLUSIONS

From the constitutive response of PBX 9501, X0242-92-4-4, and PBXN-9 measured at low- and high-strain rates and as a function of temperature at high strain rates, the following conclusions can be drawn: 1) the compressive stress-strain responses of PBX 9501, X0242-92-4-4, and PBXN-9 were found to depend strongly on both the applied strain rate (0.001 to ~2800 s^{-1}) and the test temperature (-55°C to 55°C) at high strain rates; 2) decreasing the temperature at high strain rate was found to increase the maximum flow strengths, the apparent loading modulus, and the strain-at-maximum-stress of all three energetics; and 3) from fractographic analysis PBX 9501 and X0242-92-4-4 fail at high strain rates predominantly via transgranular cleavage fracture of the HMX crystals. Measurement of various energetic formulations and pure binders is clearly necessary for the development of proper constitutive behavior and failure models.

ACKNOWLEDGMENTS

The authors acknowledge Mike Lopez, Carl Trujillo, Benny Jacquez, Chris Fugard, and Douglas Cannon for assisting with the mechanical testing and Joseph Romero for conducting the SEM. This study was conducted under the auspices of the Department of Energy and the Department of Defense/Office of Munitions, as part of the Joint DoD/DOE Munitions Technology Development Program under the Nonshock Initiation Threshold of Energetic Materials Project led by Blaine Asay. Their support is gratefully acknowledged.

REFERENCES

1. Bowden, F. P. and Gurton, O. A., "Birth and growth of explosion in liquids and solids initiated by impact and friction," Proc. R. Soc. Lond. A, vol. 198, 1949, pp. 350-372.

2. Bowden, F. P. and Yoffe, A. D., "Mechanism of initiation and growth of explosions in liquids and solids," Science of Explosives, London, 1956, pp. 539-565.

3. Belmas, R. and Plotard, J.-P., "Physical origin of hot spots in pressed explosive compositions," J. Phys. IV France Colloq. C4, vol. 5, 1995, pp. 61-87.

4. Field, J. E., "Hot spot ignition mechanisms for explosives," Accounts Chem. Res., vol. 25, 1992, pp. 489-496.

5. Field, J. E., Bourne, N. K., Palmer, S. J. P. and Walley, S. M., "Hot-spot ignition mechanisms for explosives and propellants," Phil. Trans. R. Soc. Lond. A, vol. 339, 1992, pp. 269-283.

6. Tarver, C. M., Chidester, S. K. and Nichols III, A. L., "Critical conditions for impact- and shock-induced hot spots in solid explosives," J. Phys. Chem., vol. 100, 1996, pp. 5794-5799.

7. Buntain, G. A., McKinney, T. L., Rivera, T. and Taylor, G. W., "Decomposition of energetic materials on the drop-weight-impact machine," Proc. Ninth Symposium (Int.) on Detonation, Arlington, Virginia, 1989, pp. 1037-1043.

8. Duffy, K. P. and Mellor, A. M., "A numerical study of drop weight impact testing of solid rocket propellants," Proc. 10th Int. Detonation Symposium, Arlington, Virginia, 1995, pp. 777-785.

9. Field, J. E., Swallowe, G. M. and Heavens, S. N., "Ignition mechanisms of explosives during mechanical deformation," Proc. R. Soc. Lond. A, vol. 382, 1982, pp. 231-244.

10. Metzner, A. P. and Coffey, C. S., "Hot spot initiation of plastic-bonded explosives during the rapid flow phase of the drop weight impact test," Proc. 10th Int. Detonation Symposium, Arlington, Virginia, 1995, pp. 219-223.

11. Field, J. E., Palmer, S. J. P., Pope, P. H., Sundararajan, R. and Swallowe, G. M.,

"Mechanical properties of PBX's and their behaviour during drop-weight impact," Proc. Eighth Symposium (Int.) on Detonation, White Oak, Maryland, USA, 1985, pp. 635-644.

12. Funk, D. J., Laabs, G. W., Peterson, P. D. and Asay, B. W., "Measurement of the stress/strain response of energetic materials as a function of strain rate and temperature: PBX 9501 and mock 9501," Shock Compression of Condensed Matter 1995, Woodbury, New York, 1996, pp. 145-148.

13. Hoge, K. G., "The behavior of plastic-bonded explosives under dynamic compressive loads," Appl. Polym. Symp., vol. 5, 1967, pp. 19-40.

14. Palmer, S. J. P., Field, J. E. and Huntley, J. M., "Deformation, strengths and strains to failure of polymer bonded explosives," Proc. R. Soc. Lond. A, vol. 440, 1993, pp. 399-419.

15. Peeters, R. L., "Characterization of plastic bonded explosives," J. Reinf. Plast. Compos., vol. 1, 1982, pp. 131-140.

16. Wiegand, D. A., "Constant Critical Strain for Failure of Highly Filled Polymer Composites," 3rd Int. Conf. Def. & Frac. of Composites, Univ. of Surrey, Guildford, U.K., 1995, pp. 558-567.

17. Gray III, G. T., Blumenthal, W. R., Idar, D. J. and Cady, C. M., "Influence of Temperature on the High-Strain-Rate Mechanical Behavior of PBX 9501," Shock Compression of Condensed Matter - 1997, 1997, pp. in press.

18. Gray III, G. T., Blumenthal, W. R., Trujillo, C. P. and Carpenter II, R. W., "Influence of temperature and strain rate on the mechanical behavior of Adiprene L-100," J. Phys. IV France Colloq. C3 (EURODYMAT 97), vol. 7, 1997, pp. 523-528.

19. Follansbee, P. S. and Frantz, C., "Wave propagation in the SHPB," Trans. ASME: J. Engng Mater. Technol., vol. 105, 1983, pp. 61-66.

20. Walley, S. M. and Field, J. E., "Strain rate sensitivity of polymers in compression from low to high strain rates," DYMAT Journal, vol. 1, 1994, pp. 211-228.

21. Idar, D. J., Peterson, P. D., Scott, P. D. and Funk, D. J., "Low Strain Rate Compression Measurements of PBXN-9, PBX 9501, AND Mock 9501," 1997 APS Topical Conference on Shock Compression of Condensed Matter, Amherst, MA, July 28 - Aug. 1, 1997 (in press).

"Adhesives Technology of Estane Polyurethane," B. F. Goodrich Technical Service Report TSR 76-02 TF 116, B. F. Goodrich Speciality Chemicals, Cleveland, OH (March 1995.)

Baulder, B., Hutcheson, R., Gallant, M., and Leahy, J. " Characterization of PBXW-9," Naval Surface Warfare Center Report NSWC TR 86-334, Dahlgren, VA and Silver Spring, MD (August 1989.)